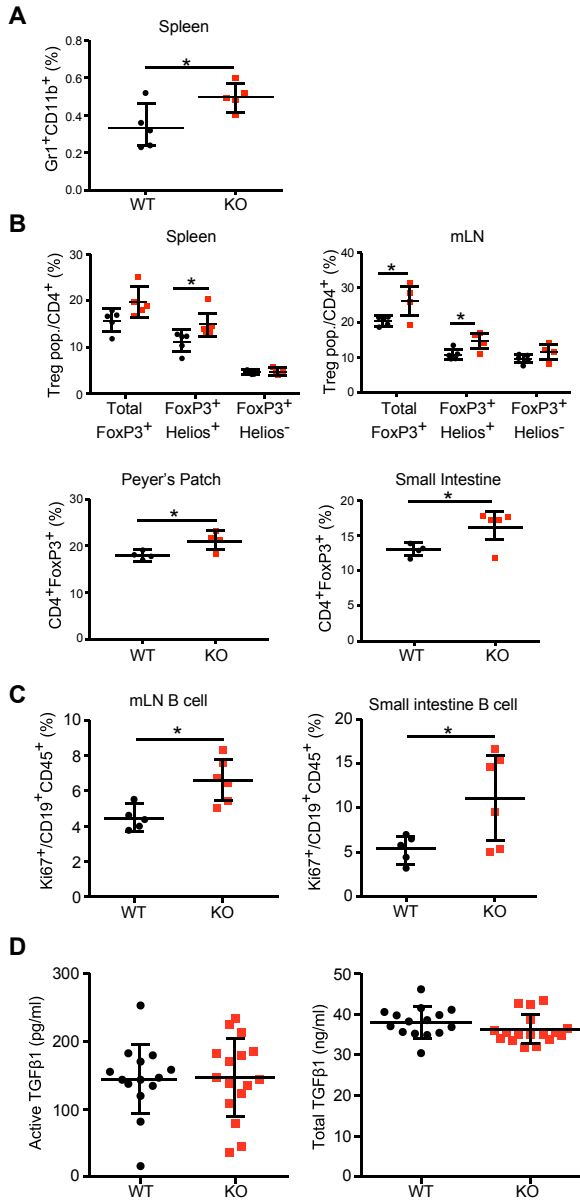
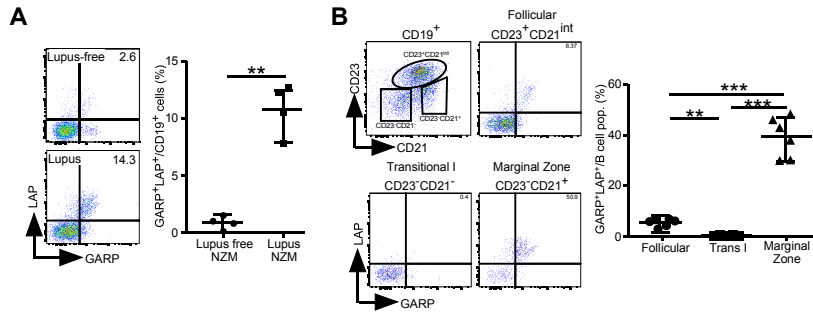


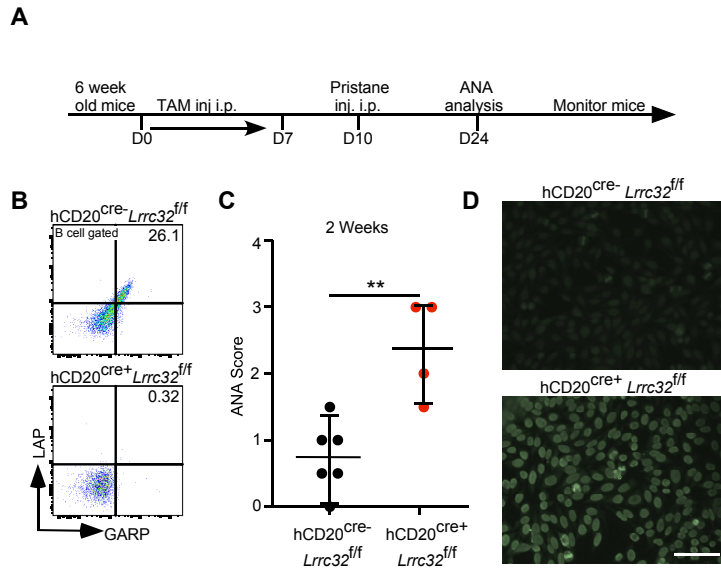
## Supplemental Figures



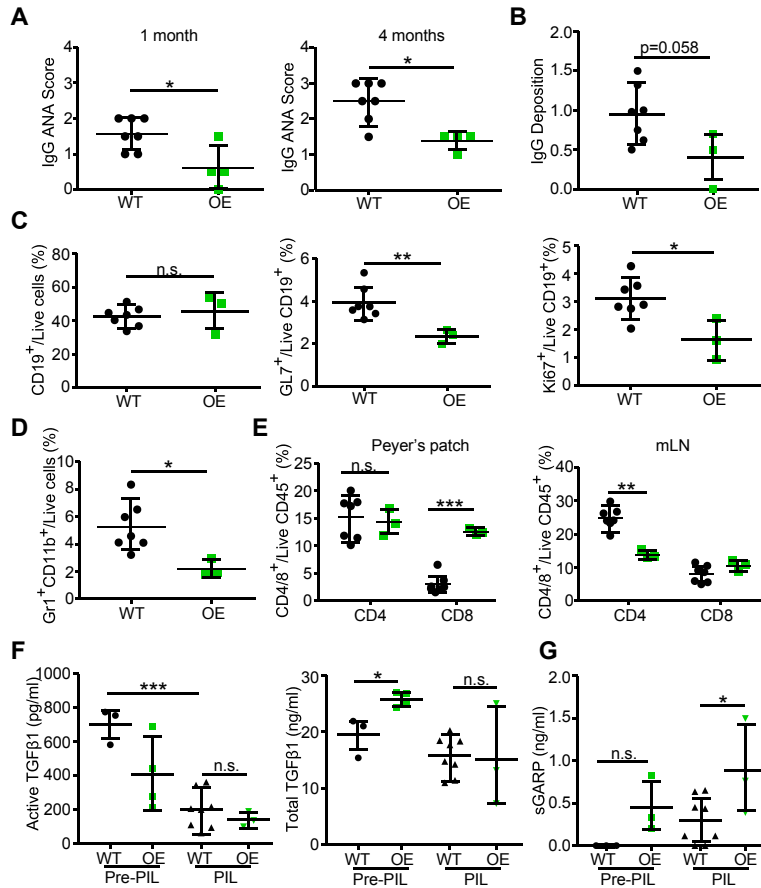
**Supplemental Figure 1: Changes in other immune compartments and increased mucosal B cell proliferation in B cell *Lrrc32* deficient BM chimera mice.** Immune compartments were analyzed in BM chimera mice 6 months post BM reconstitution. **(A)** Live Gr1<sup>+</sup>CD11b<sup>+</sup> granulocytic cells were detected in the spleen by flow,  $n=5$  biological replicates. **(B)** Total FoxP3<sup>+</sup> Tregs and Helios<sup>+/−</sup> Tregs were detected in the spleen ( $n=5$ ), mesenteric lymph nodes (mLN;  $n=5$ ), Peyer's patch ( $n=4$ ), and small intestine lamina propria ( $n=4-5$ ) by flow cytometry. **(C)** Immune cells were isolated from the mLN and small intestine, and stained for CD19 to detect B cells and intracellularly for Ki67, followed by flow cytometry analysis ( $n=5-6$  WT and KO mice). **(D)** Active and total TGF- $\beta$  levels were measured by ELISA in WT and GARP KO BM chimera mice 6 months post BM reconstitution. Statistics performed by two-tailed  $t$ -test; \*  $p<0.05$ , error bars represent S.D.



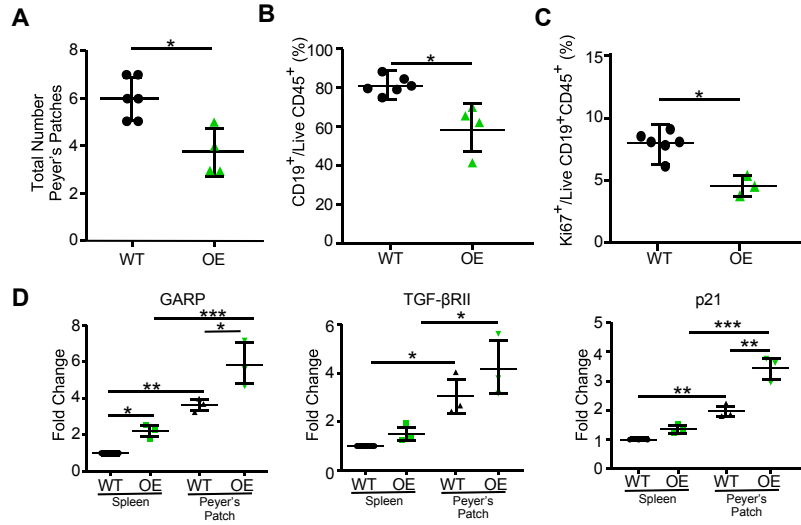
**Supplemental Figure 2: B cell GARP in murine lupus models.** (A) Representative flow plots of GARP and LAP expression gated on live total splenic CD19<sup>+</sup> B cells from NZM2410 mice with (Lupus) and without (Lupus-free) active lupus and the quantification of the data (right),  $n=4$ , representative of two independent experiments. Statistical analysis performed by two-tailed  $t$ -test, \*\*  $p<0.01$ , error bars represent S.D. (B) Flow plots depicting GARP and LAP surface expression on live splenic CD19<sup>+</sup> follicular B cells (CD23<sup>+</sup>CD21<sup>int</sup>), marginal zone B cells (CD23<sup>-</sup>CD21<sup>+</sup>), and transitional I B cells (CD23<sup>-</sup>CD21<sup>-</sup>) from lupus NZM2410 mice and the quantification of the data (right),  $n=6$ , representative of two independent experiments. Statistical analysis performed by one-way ANOVA with Tukey's test for multiple comparisons, \*\*  $p<0.01$ , \*\*\*  $p<0.001$ , error bars represent S.D.



**Supplemental Figure 3: hCD20-ER<sup>cre</sup> Lrrc32<sup>ff</sup> B cell specific GARP deficient mice have an increase in early onset PIL.** Female WT and hCD20-ER<sup>cre</sup> Lrrc32<sup>ff</sup> B cell GARP KO mice were injected with Tamoxifen for 7 days to delete GARP, WT ( $n=6$ ) and GARP OE ( $n=4$ ) mice. **(A)** Scheme of GARP deletion with Tamoxifen and subsequent pristane injection to induce autoimmunity. **(B)** Mice were bled 8 days after Tamoxifen injection and peripheral blood was cultured with LPS for 48 hours to induce GARP. Cells were stained with CD19, GARP, and LAP and analyzed by flow cytometry to confirm GARP deletion in KO mice. **(C and D)** Two weeks after pristane injection, sera were collected and ANA was measured. Representative images shown in **D**. Data are representative of two independent experiments. Statistical analysis performed by unpaired two-tailed  $t$ -test; \*\*  $p < 0.01$ , error bars represent S.D.



**Supplemental Figure 4: GARP overexpression dampens pristane-induced autoimmunity in mice.** rtTA GARP OE mice were fed doxycycline in the drinking water one week prior to a single intraperitoneal pristane injection. Doxycycline treatment was continued throughout the course of the experiment for both GARP WT ( $n=7$ ) and GARP OE ( $n=4$ ) mice. **(A)** IgG ANA levels were measured in the serum of pristane treated mice at 1 month and 4 months post pristane injection. **(B)** Five  $\mu\text{m}$  thick kidney sections were stained with anti-IgG-FITC to detect immunoglobulin deposition in the glomeruli. Data shown are the quantification;  $n=7$  WT and  $n=3$  OE (one OE mice died prior to analysis). **(C)** Immune cells were isolated from the spleen and percentages of B cells (CD19<sup>+</sup>), germinal center B cells (GL7<sup>+</sup>CD19<sup>+</sup>), and Ki67<sup>+</sup> B cells from WT and OE mice were quantified. **(D)** MDSCs (Gr1<sup>+</sup>CD11b<sup>+</sup>) in pristane treated WT and OE mice were quantified. **(E)** Peyer's patch and mesenteric lymph node (mLN) immune cells were isolated and percentages of CD4 T cells and CD8 T cells were quantified. **(F)** Active and total TGF- $\beta$ 1 levels were measured in the sera of WT and GARP OE mice pre- and post-PIL by ELISA. **(G)** Soluble GARP (sGARP) was measured in the sera of WT and GARP OE mice pre- and post-PIL by ELISA.  $n=3$  WT and  $n=4$  OE Pre-PIL;  $n=7$  WT and  $n=3$  OE post-PIL. Statistical analysis performed by unpaired two-tailed  $t$ -test; \*  $p<0.05$ , \*\*  $p<0.01$ , \*\*\*  $p<0.001$ , error bars represent S.D.



**Supplemental Figure 5: GARP overexpression reduces Peyer's patch B cell cellularity and proliferation.** rtTA GARP OE and control WT mice were both fed doxycycline in the drinking water for 4 months,  $n=6$  WT and  $n=3-4$  OE. **(A)** Total number of Peyer's patches on the small intestine were counted. **(B)** Peyer's patches were isolated and percentage of CD19<sup>+</sup> B cells was analyzed by flow cytometry. **(C)** Peyer's patch B cells were stained intracellularly for Ki67 to assess homeostatic proliferation and analyzed by flow cytometry. Each dot is representative of a separate biological replicate; data is representative of 3 independent experiments. **(A-C)** Statistical analysis performed by two-tailed *t*-test; \*  $p < 0.05$ , error bar represents S.D. **(D)** CD19<sup>+</sup> B cells were isolated from the spleen and Peyer's patches of Doxycycline treated WT and GARP OE mice, followed by RNA isolation and cDNA synthesis. qRT PCR was utilized to detect differences in GARP, TGF- $\beta$ RII and p21 transcript level, normalized to  $\beta$ -actin. Representative data from 3 independent experiments with 3 biological replicates. Statistical analysis performed by one-way ANOVA with Tukey's test for multiple comparisons, \*  $p < 0.05$ , \*\*  $p < 0.01$ , \*\*\*  $p < 0.001$ , error bars represent S.D.